

# A limit on the electron electric dipole moment using paramagnetic ferroelectric $\text{Eu}_{0.5}\text{Ba}_{0.5}\text{TiO}_3$

S. Eckel,\* A.O. Sushkov,† and S.K. Lamoreaux  
 Yale University, P.O. Box 208120 New Haven, CT 06520-8120  
 (Dated: January 24, 2018)

We report on the results of a search for the electron electric dipole moment  $d_e$  using paramagnetic ferroelectric  $\text{Eu}_{0.5}\text{Ba}_{0.5}\text{TiO}_3$ . The electric polarization creates an effective electric field that makes it energetically favorable for the spins of the seven unpaired  $4f$  electrons of the  $\text{Eu}^{2+}$  to orient along the polarization, provided that  $d_e \neq 0$ . This interaction gives rise to sample magnetization, correlated with its electric polarization, and is therefore equivalent to a linear magnetoelectric effect. A SQUID magnetometer is used to search for the resulting magnetization. We obtain  $d_e = (-1.07 \pm 3.06_{\text{stat}} \pm 1.74_{\text{sys}}) \times 10^{-25} \text{ ecm}$ , implying an upper limit of  $|d_e| < 6.05 \times 10^{-25} \text{ ecm}$  (90% confidence).

PACS numbers: 11.30.Er, 75.85.+t, 32.10.Dk, 14.60.Cd

The permanent electron electric dipole moment ( $e\text{EDM}$ ) has been of experimental interest for nearly half a century because it provides a probe of charge-parity (CP) symmetry violation in the universe. Through the CPT theorem [1], the existence of a permanent electric dipole moment, which violates time-reversal (T) symmetry, would imply violation of CP in order that combined operations of CPT are conserved. CP symmetry violation is required in the early universe in order to explain the currently observed matter-antimatter asymmetry [2]; furthermore, the CP violation in the standard model (SM) is not sufficient to explain this asymmetry [3]. Many theories that go beyond the SM contain more CP violation and therefore predict a larger  $e\text{EDM}$  that may be detected by the next generation of experiments [4].

The traditional method to search for an  $e\text{EDM}$  involves observing precession of an atom or molecule with unpaired electron spins in the presence of both magnetic and electric fields [5]. This method has been used extensively [6, 7] and has set the best current upper limit on the  $e\text{EDM}$  of  $|d_e| < 1.05 \times 10^{-27} \text{ ecm}$  [8]. Another measurement procedure, first suggested by Shapiro [9], involves placing unpaired electron spins bound to a crystal lattice in an electric field. If  $d_e \neq 0$ , the electrons will orient along the electric field and produce a magnetization in the sample [10]. To date, two experiments produced  $e\text{EDM}$  limits using this approach [11, 12]. The reverse experiment, where the sample is magnetized and a correlated polarization is measured, has also been performed [13]. These solid-state-based experiments sacrifice the narrow atomic and molecular transition linewidths for a significantly larger signal due to the high density of spins present in a solid.

Perhaps the most important choice for a solid-state  $e\text{EDM}$  experiment is the material. In Refs. [14, 15], the advantages of  $\text{Eu}_{0.5}\text{Ba}_{0.5}\text{TiO}_3$  are detailed over other materials, and a short review will be presented here.  $\text{Eu}_{0.5}\text{Ba}_{0.5}\text{TiO}_3$  has a perovskite crystal structure and is ferroelectric below approximately 200 K [14, 16, 17]. Our samples, which have approximately 65% ceramic density and were made in an identical way to those in Ref. [15], can be partially polarized using moderate voltage ( $\leq 3 \text{ kV}$  or approximately 20 kV/cm). The magnetic  $\text{Eu}^{2+}$  ions are responsible for paramagnetic behav-

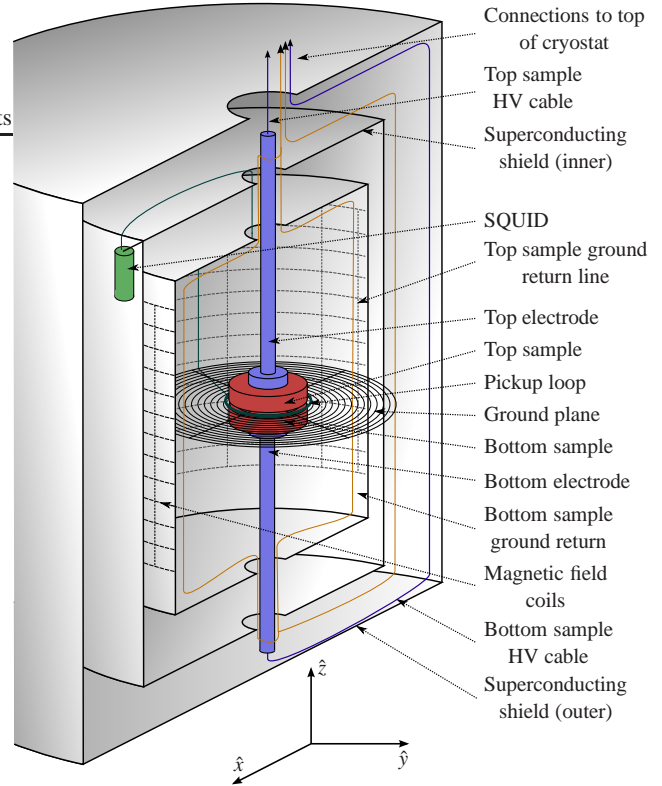


FIG. 1. (Color online) A cut-through schematic of the  $e\text{EDM}$  experiment. Note the coordinate system in the bottom of the figure.

ior above approximately 1.9 K and behavior consistent with anti-ferromagnetism at lower temperatures [14].

The sample magnetization induced by the  $e\text{EDM}$  is given by

$$M = \frac{\chi_m d_e E^*}{\mu_a}, \quad (1)$$

where  $\chi_m$  is the magnetic susceptibility,  $d_e$  is the  $e\text{EDM}$  of the electron,  $\mu_a$  is the magnetic moment of the  $\text{Eu}^{2+}$  ion, and  $E^*$  is the effective electric field. As shown for a similar, dielectric material,  $\text{Gd}_3\text{Ga}_5\text{O}_{12}$ , the effective electric field is proportional to the displacement of the  $\text{Eu}^{2+}$  with respect to the

center of the oxygen octahedron around it [18]. This displacement has been computed to be equal to half that of the displacement of the  $\text{Ti}^{4+}$  ions with respect to the  $\text{O}^{2-}$  [14] and is therefore proportional to the polarization of the sample, i.e.,  $E^* = kP$ . Using this displacement and the results in Ref. [18], we conservatively predict  $k \approx (10 \text{ MV/cm})/(1 \mu\text{C/cm}^2)$ . The EDM interaction [Eq. 1] can be viewed as a first order, linear magnetoelectric (ME) effect in the sample. In this picture, the free energy of the sample  $\tilde{\Phi}$  is modified by a linear term  $\alpha'HP$ , where  $\alpha' = \chi_m d_{ek}/\mu_a$  and  $H$  is the applied magnetic field. Because the sample is cooled in a zero electric field and the experiment is operated at 4.2 K where the sample is paramagnetic, both parity and time symmetries are conserved in the crystal. A non-zero  $\alpha'$  can therefore only arise because of the  $e$ EDM [19].

A cut-through schematic of the experimental apparatus is shown in Fig. 1. Two disc-shaped samples of diameter 12.6 mm and height 1.7 mm are held onto a centrally located ground plane by two electrodes. Like most of the cryogenic components, the ground plane is constructed from G10 fiberglass but is coated with graphite to make the surface conductive. An 8-turn superconducting Nb-Ti alloy pickup loop is wound inside the ground plane. The pickup loop transfers the flux generated by the magnetization of the samples to a superconducting quantum interference device (SQUID) that is used as a magnetometer. Because of the geometry of the samples, there are demagnetizing fields that lead to suppression of the magnetic flux detected by the SQUID [20]. To electrically polarize the samples, voltage is generated by a custom-built high voltage supply and applied via graphite-painted electrodes on the flat surfaces of the samples. Additional leads from the ground planes attach to a high dynamic range, transimpedance amplifier [21], with which currents that flow through the sample are measured. The polarization is determined by numerically integrating the measured current. Such numerical integration is accurate only to an arbitrary constant and thus measures the change in polarization but not the *absolute* polarization.

Two layers of superconducting magnetic shields made of 1 mm thick, 99.9% pure Pb foil surround the sample region. This shielding offers a minimum shielding factor of  $10^8$  for time-varying magnetic fields. However, during cooling of the experiment, they trap ambient magnetic fields as they undergo the superconducting transition. This trapped field can be canceled using superconducting magnetic field coils wound on a cylindrical form of radius 5.2 cm and length 17 cm. A solenoid coil applies a field  $H_z$  parallel to the normal vector of the pickup loop (defined to be the  $\hat{z}$  direction), and a cosine- $\theta$  type coil applies a field  $H_x$  perpendicular to the normal vector of the pickup loop at a set azimuthal angle (defined to be the  $\hat{x}$  direction). Lastly, an anti-Helmholtz coil applies a magnetic field gradient  $dH_z/dz$ .

Fig. 2 shows the experimental measurement procedure. Electric field pulses separated by a time  $\tau$  are applied to either the top sample, bottom sample, or both to modulate the remanent polarization. Because Eq. 1 is linear in  $P$ , the  $e$ EDM-

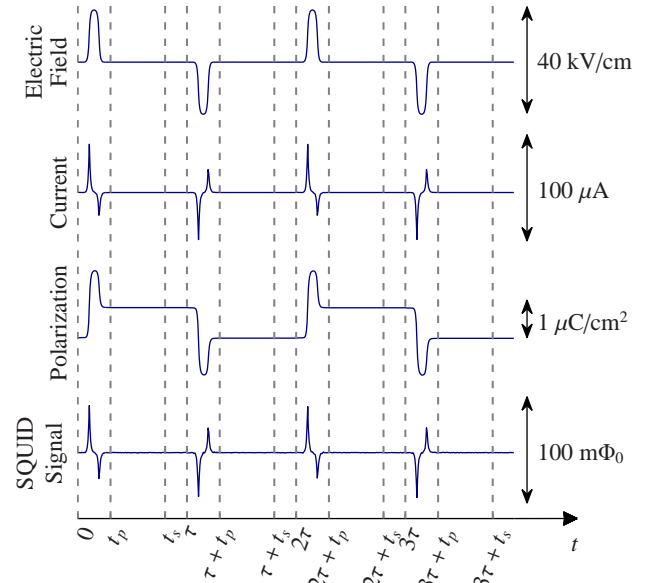


FIG. 2. (Color online) The procedure for measuring the  $e$ EDM. Electric field pulses (top) of duration  $t_p$  are applied a time  $\tau$  apart. Each subsequent pulse reverses the polarization of the sample. The current flow through the samples (second from the top) is numerically integrated to obtain the polarization of the samples (second from the bottom). The SQUID signal (bottom) is averaged after each pulse between times  $t_s$  and  $\tau$ , where  $t_s$  is generally  $0.8\tau$ . Shown on the right are typical orders of magnitude for the various applied fields and measured quantities. If  $d_e \approx 10^{-27}$  ecm, the size of the SQUID signal would be of order  $1 \text{ n}\Phi_0$ .

induced magnetization will be similarly modulated. To measure the resulting modulation, the SQUID signal is averaged after allowing time for transients to settle. To prevent background drifts in the signal from impacting the computation of the correlation, the average SQUID signals for four adjacent pulses in time are weighted by  $\frac{1}{4}$ ,  $-\frac{3}{4}$ ,  $\frac{3}{4}$ ,  $-\frac{1}{4}$  and summed. This procedure determines the difference in the SQUID signal between the two polarization states  $\Delta\Phi$  and eliminates the effect of a linear drift.  $\Delta\Phi$  is then divided by the difference in the polarization  $\Delta P$  to determine the correlation between the SQUID signal and the polarization. This correlation  $\Delta\Phi/\Delta P$  is proportional to the ME coefficient  $\alpha'$  and thus  $d_e$ .

The predominant noise source is the SQUID magnetometer's intrinsic noise. Above 1 Hz, the noise spectral density is approximately white at  $3 \mu\Phi_0/\sqrt{\text{Hz}}$ . Below 1 Hz, the noise of the SQUID rises roughly as  $1/f$ , where  $f$  is the frequency. Due to technical constraints, the fastest  $\tau$  corresponds to a reversal frequency of 0.25 Hz, within the  $1/f$  noise regime of our SQUIDs. Despite operating in the  $1/f$  regime of the noise, the statistics for a data run are Gaussian. Each data run comprises between 200 and 600 electric field pulses, and a Gaussian is fit to the distribution of  $\Delta\Phi/\Delta P$ . The error of the best fit mean is used as the statistical error for that run. The typical reduced  $\chi^2$  for such a fit is near unity. Because the samples are reversed at a frequency within the  $1/f$  noise regime of the

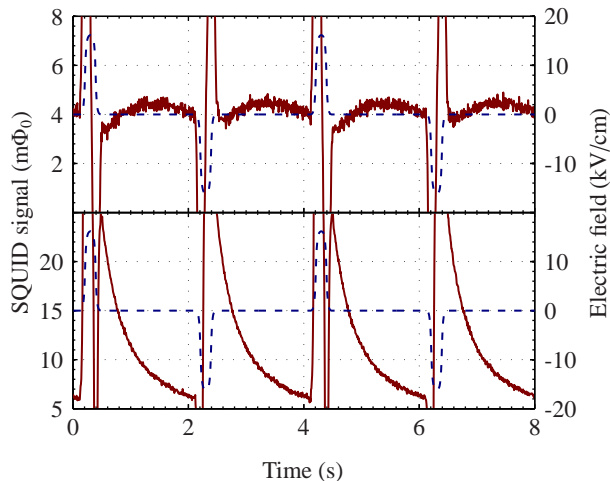


FIG. 3. (Color online) Example of the difference of the heating decay transient. The blue dashed lines show the applied electric field pulses and the red solid lines show the resulting SQUID signal. The large features in the SQUID signal seen during the electric field pulses are caused by the current that flows during the polarization reversal. After the reversal, the heated sample returns to equilibrium with the LHe bath, which can be seen as the decay after the pulse. These data were taken in the presence of an  $H_x$  field (top panel) and an  $H_z$  field (bottom panel), each approximately 1 mG.

137 SQUIDS, the statistical errors of  $\Delta\Phi/\Delta P$  tend to be an order  
138 of magnitude larger than those projected in Ref. [15].

139 Several systematic effects in the experiment can generate a  
140 non-zero  $\Delta\Phi/\Delta P$  and can therefore mask or mimic the linear  
141 ME effect due to the  $e$ EDM. For example, if the samples are  
142 in a non-zero magnetic field, a change in the temperature of  
143 the sample(s) will lead to a change in permeability that will  
144 subsequently change the flux through the SQUID. Because of  
145 the dissipation inherent to ferroelectrics, polarization reversals  
146 heat the sample(s). As the samples return to equilibrium with  
147 the liquid helium bath, a transient can be seen in the SQUID  
148 signal, as shown in Fig. 3. Provided this heating is equal when  
149 the sample polarization is switched from  $+\hat{z}$  to  $-\hat{z}$  (a negative  
150 pulse) and  $-\hat{z}$  to  $+\hat{z}$  (a positive pulse), the heating transients  
151 are identical for positive and negative remanent polarizations,  
152 and there is no systematic effect. A measure of the amount of  
153 heat released by a given pulse can be derived from the integral  
154 of  $P \cdot dE$ , where  $P$  is the polarization and  $E$  is the applied  
155 electric field [22], and is of the order of 1 mJ per pulse.

156 To quantify the size of the resulting  $\Delta\Phi/\Delta P$ , magnetic fields  
157 were applied and the electric field pulses were deliberately  
158 unbalanced to produce different heating for positive and nega-  
159 tive pulses. The resulting correlation was measured in this  
160 manner for each reversal frequency and for each sample. The  
161 correlations were then fit to  $\Delta\Phi/\Delta P = a\Delta Qp$ , where  $\Delta Q$  is  
162 the difference in heat released between a positive and negative  
163 pulse,  $p$  is a proxy for the magnetic field, and  $a$  is a tunable  
164 constant. As shown in Fig. 3, the transient is significantly dif-  
165 ferent for  $H_x$  vs.  $H_z$  fields; for this reason, the fits for the  
166 correlation use  $p = \langle d^2\Phi/dt^2 \rangle$  as a proxy for the strength of  $H_z$

167 and  $p = \langle d^2\Phi/dt^2 \rangle$  as a proxy for the strength of  $H_x$ . The re-  
168 sulting fits to experimental data confirm the validity of these  
169 proxies. The best fit values for  $a$  are used to predict the size  
170 of the correlation when the magnetic field is close to zero and  
171 the electric field pulses are symmetric. In this configuration, it  
172 is not known *a priori* what type of field envelops the samples;  
173 therefore, the most likely correlation for both an  $H_z$  field and  
174 an  $H_x$  field is computed. The resulting predictions are used as  
175 a  $1-\sigma$  systematic error without applying any correction.

176 In addition to this heating effect, the higher-order ME ef-  
177 fect that is present in titanates can also generate a non-zero  
178  $\Delta\Phi/\Delta P$ . Given the symmetries present in our sample, the  
179 magnetization induced by the higher-order ME effect will be  
180 given by  $M = \delta\chi_m P^2 H$ , where  $P$  is the *absolute* polarization.  
181 Using the same experimental apparatus, the constant  $\delta$  was  
182 measured for this material; details will be presented in a later  
183 paper in preparation. Because the magnetoelectric-induced  
184 magnetization depends on  $P^2$ , a non-zero correlation will re-  
185 sult only if the two different absolute polarization states in the  
186 modulation have different magnitudes. Thus, the error in de-  
187 termining the absolute zero of polarization will determine the  
188 maximum possible difference in  $P^2$  when the polarization is  
189 reversed. The error in the absolute zero of  $P$  is taken to be  
190  $0.1 \mu\text{C}/\text{cm}^2$  at 95% confidence, which is motivated by the fi-  
191 delity with which samples can be depolarized using electric  
192 fields. Depolarization effectively resets the constant of inte-  
193 gration in the determination of the polarization and thus the  
194 fidelity limits our knowledge of the absolute zero of the po-  
195 larization. Using this error estimate for the absolute measure-  
196 ment of  $P$ , a  $\Delta\Phi/\Delta P$  is computed and used as a systematic  
197 error.

198 Because of the inherent dissipation present in ferroelectrics,  
199 the sample takes some time to reach the final polarization state  
200 after the electric field is applied. This phenomenon is known  
201 as dielectric relaxation [23]. As the sample relaxes to its fi-  
202 nal state, current continues to flow through the sample. This  
203 current scales as  $t^{-1}$ , where  $t$  is the time since the polariza-  
204 tion reversal. To suppress this dielectric relaxation, an addi-  
205 tional time-varying voltage (maximum 40 V) is applied using  
206 a proportional-integrator-differentiator (PID) circuit to force  
207 the net current to zero. To estimate a  $\Delta\Phi/\Delta P$  that may result,  
208 the SQUID response during the electric field pulse is used to  
209 calculate the sensitivity of the SQUID to the current through  
210 each sample. The effect on the SQUID signal due to any cur-  
211 rent that is not suppressed by the PID is then computed and  
212 used to estimate the correlation. The correlation due to di-  
213 electric relaxation is then taken to be a  $1-\sigma$  systematic error.

214 The total integrated time for the data used in the final analy-  
215 sis is approximately 1 hour and 40 minutes. All data where the  
216 same sample(s) are driven at the same reversal frequency and  
217 with the same amplitude electric field pulses were averaged  
218 together, weighted by their statistical errors. The correlation  
219 is then converted into a linear ME coefficient and an equiv-  
220 alent  $d_e$ . To enable comparison with linear ME coefficients  
221 that are expressed in units of  $\text{s m}^{-1}$ , we define  $\alpha = \chi_e \epsilon_0 \alpha'$ ,  
222 where  $\chi_e = P/\epsilon_0 E \approx 700$  is an effective electrical susceptibil-

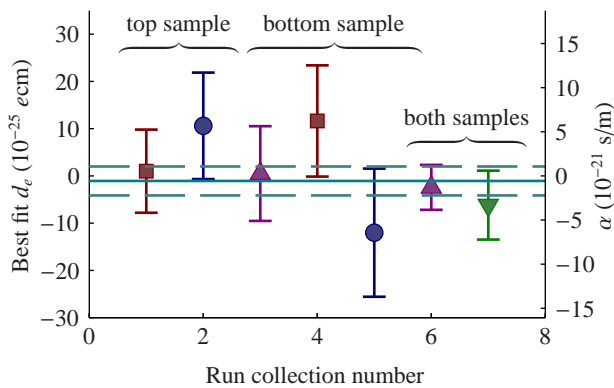


FIG. 4. (Color online) Final best fit  $e$ EDM values with statistical error bars. Data were recorded at reversal frequencies of 0.25 Hz (violet, upward triangles), 0.167 Hz (red squares), 0.125 Hz (green, downward triangles), and 0.1 Hz (blue circles). The annotations show which sample(s) were driven. The solid cyan line shows the best fit mean, and the dashed cyan lines show its  $1\text{-}\sigma$  statistical error.

	Top	Bottom	Both
Heating ( $H_x$ )	0.71	1.82	-0.07
Heating ( $H_z$ )	-0.05	-0.72	-0.02
Dielectric relaxation	-0.97	-0.11	0.70
Higher-order ME effect	1.40	0.26	0.47

TABLE I. Breakdown of the systematic errors in the experiment by source and which sample(s) were driven. Units of the table are  $10^{-25}$  ecm.

ity for the ferroelectric. The results are shown in Fig. 4 and are consistent with zero.

A breakdown of the systematics is shown in Tab. I. The higher-order ME effect produces a significant systematic effect because of the conservative estimate of our knowledge of the absolute polarization. The systematic due to the heating shows complicated behavior, and is significantly less when both samples are driven. The reason for this reduction is twofold. When driving both samples, there is a significant rejection of the effect of a transverse field because  $H_x$  couples to the two samples in the opposite way. Second, the asymmetry in the heating when both samples were used was measured to be nearly equal and opposite, leading to rejection of  $H_z$ .

The final best fit results are  $d_e = (-1.07 \pm 3.06_{\text{stat}} \pm 1.74_{\text{sys}}) \times 10^{-25}$  ecm and  $\alpha = (-0.57 \pm 1.64_{\text{stat}} \pm 0.93_{\text{sys}}) \times 10^{-21}$  s/m [24]. This result implies an  $e$ EDM limit of  $|d_e| < 6.05 \times 10^{-25}$  ecm (90% confidence). Compared to previous solid state  $e$ EDM measurements, this limit is approximately a factor of ten improvement over Ref. [13] and a factor of three better than Ref. [12].

In conclusion, we have built and operated an experiment that has established an upper limit on the  $e$ EDM better than any previously published solid-state experiment. The typical remanent polarization of  $\text{Eu}_{0.5}\text{Ba}_{0.5}\text{TiO}_3$  of  $0.5 \mu\text{C}/\text{cm}^2$  offers a large effective electric field that interacts with the EDM, approximately 700 times larger than that obtained in Ref. [12]

where dielectric  $\text{Gd}_3\text{Ga}_5\text{O}_{12}$  was used. The ultimate EDM limit can be improved in future versions of the experiment by identifying and suppressing the sources of excess noise in the SQUID magnetometers below 1 Hz. Further suppression of systematics, such as heating and dielectric relaxation, could be obtained by improving magnetic shielding and optimizing the current feedback system. Alternatively, these systematics may be suppressed by using either a low-loss ferroelectric (e.g.,  $\text{Eu}_{0.5}\text{Ba}_{0.25}\text{Sr}_{0.25}\text{TiO}_3$  [25]) or paraelectric (e.g.,  $\text{SrTiO}_3$  doped with  $\text{Eu}^{2+}$  [26, 27]).

The authors would like to thank N.A. Spaldin, O.P. Sushkov, D. Budker, L.S. Bouchard and D.P. DeMille for useful discussions. We would also like to thank J. Haase, N. Georgieva, S. Kamba for providing preliminary measurements of  $\text{Eu}_{0.5}\text{Ba}_{0.5}\text{TiO}_3$ . This work was supported by Yale University.

\* stephen.eckel@aya.yale.edu; Present Address: Joint Quantum Institute, National Institute of Standards and Technology, Gaithersburg, MD 20899, USA

† Present Address: Physics Department, Harvard University, Cambridge, Massachusetts 02138, USA

- [1] J. Schwinger, *Physical Review* **82**, 914 (1951)
- [2] A. D. Sakharov, *Pisma Zh. Eksp. Teor. Fiz.* **5**, 32 (1967)
- [3] G. R. Farrar and M. E. Shaposhnikov, *Physical Review D* **50**, 774 (1994)
- [4] W. Bernreuther and M. Suzuki, *Reviews of Modern Physics* **63**, 313 (Apr 1991)
- [5] I. B. Khriplovich and S. K. Lamoreaux, *CP Violation without Strangeness* (Springer-Verlag, Berlin, 1997)
- [6] B. C. Regan, E. D. Commins, C. J. Schmidt, and D. DeMille, *Phys. Rev. Lett.* **88**, 071805 (Feb 2002)
- [7] W. C. Griffith, M. D. Swallows, T. H. Loftus, M. V. Romalis, B. R. Heckel, and E. N. Fortson, *Phys. Rev. Lett.* **102**, 101601 (2009)
- [8] J. J. Hudson, D. M. Kara, I. J. Smallman, B. E. Sauer, M. R. Tarbutt, and E. A. Hinds, *Nature* **473**, 493 (2011)
- [9] F. L. Shapiro, *Soviet Physics Uspekhi* **11**, 345 (1968)
- [10] D. Budker, S. K. Lamoreaux, A. O. Sushkov, and O. P. Sushkov, *Physical Review A* **73**, 022107 (2006)
- [11] B. V. Vasil'ev and E. V. Kolycheva, *Sov. Phys. JETP* **47**, 243 (1978)
- [12] Y. J. Kim, C. Y. Liu, S. K. Lamoreaux, and G. Reddy, *Journal of Physics: Conference Series* **312**, 102009 (2011)
- [13] B. J. Heidenreich, O. T. Elliott, N. D. Charney, K. A. Virgien, A. W. Bridges, M. A. McKeon, S. K. Peck, J. D. Krause, J. E. Gordon, L. R. Hunter, and S. K. Lamoreaux, *Physical Review Letters* **95**, 253004 (2005)
- [14] K. Z. Rushchanskii, S. Kamba, V. Goian, P. Vaněk, M. Savinov, J. Prokleška, D. Nuzhnyy, K. Knížek, F. Laufek, S. Eckel, S. K. Lamoreaux, A. O. Sushkov, M. Ležaić, and N. A. Spaldin, *Nature Materials* **9**, 649 (2010)
- [15] A. O. Sushkov, S. Eckel, and S. K. Lamoreaux, *Physical Review A* **81**, 022104 (2010)
- [16] W. N. Rowan-Weetaluktuk, D. H. Ryan, A. O. Sushkov, S. Eckel, S. K. Lamoreaux, O. P. Sushkov, J. M. Cadogan, M. Yethiraj, and A. J. Studer, *Hyperfine Interactions* **198**, 1 (2010)

- 306 [17] V. Goian, S. Kamba, D. Nuzhnyy, P. Vaněk, M. Kempa, V. Bov- 318  
307 tun, K. Knížek, J. Prokleška, F. Borodavka, M. Ledinský, and 319  
308 I. Gregora, *Journal of Physics: Condensed Matter* **23**, 025904 320  
309 (2011) 321
- 310 [18] T. N. Mukhamedjanov, V. A. Dzuba, and O. P. Sushkov, 322  
311 *Physical Review A* **68**, 042103 (2003) 323
- 312 [19] G. A. Smolenskiĭ and I. E. Chupis, *Soviet Physics Uspekhi* **25**, 324  
313 475 (1982) 325
- 314 [20] A. O. Sushkov, S. Eckel, and S. K. Lamoreaux, 326  
315 *Physical Review A* **79**, 022118 (2009) 327
- 316 [21] S. Eckel, A. O. Sushkov, and S. K. Lamoreaux, 328  
317 *Review of Scientific Instruments* **83**, 026106 (2012) 329
- 318 [22] J. D. Jackson, *Classical Electrodynamics*, 3rd ed. (John Wiley 319  
and Sons, Hoboken, 1999)
- 320 [23] A. K. Jonscher, *Journal of Physics D: Applied Physics* **32**, R57 321  
(1999)
- 322 [24] The error in  $d_e$  does not include any uncertainty from the theo- 323  
retical estimate of  $E^*$ .
- 324 [25] V. Goian, S. Kamba, P. Vanek, M. Savinov, C. Kadlec, and 325  
J. Prokleska, *ArXiv e-prints*(2012), arXiv:1208.2551
- 326 [26] K. A. Müller and H. Burkard, *Physical Review B* **19**, 3593 327  
(1979)
- 328 [27] R. Viana, P. Lunkenheimer, J. Hemberger, R. Böhmer, and 329  
A. Loidl, *Physical Review B* **50**, 601 (1994)